Cross-Species Mechanical Fingerprinting of Cardiac Myosin Binding Protein-C

Árpád Karsai,[†] Miklós S. Z. Kellermayer,[‡§] and Samantha P. Harris[†*]
[†]University of California - Davis, Davis, California; [‡]MTA-SE Molecular Biophysics Research Group and [§]Department of Biophysics and Radiation Biology, Semmelweis University, Budapest, Hungary

ABSTRACT Cardiac myosin binding protein-C (cMyBP-C) is a member of the immunoglobulin (Ig) superfamily of proteins and consists of 8 Ig- and 3 fibronectin III (FNIII)-like domains along with a unique regulatory sequence referred to as the MyBP-C motif or M-domain. We previously used atomic force microscopy to investigate the mechanical properties of murine cMyBP-C expressed using a baculovirus/insect cell expression system. Here, we investigate whether the mechanical properties of cMyBP-C are conserved across species by using atomic force microscopy to manipulate recombinant human cMyBP-C and native cMyBP-C purified from bovine heart. Force versus extension data obtained in velocity-clamp experiments showed that the mechanical response of the human recombinant protein was remarkably similar to that of the bovine native cMyBP-C. Ig/Fn-like domain unfolding events occurred in a hierarchical fashion across a threefold range of forces starting at relatively low forces of ~50 pN and ending with the unfolding of the highest stability domains at ~180 pN. Force-extension traces were also frequently marked by the appearance of anomalous force drops suggestive of additional mechanical complexity such as structural coupling among domains. Both recombinant and native cMyBP-C exhibited a prominent segment ~100 nm-long that could be stretched by forces <50 pN before the unfolding of Ig- and FN-like domains. Combined with our previous observations of mouse cMyBP-C, these results establish that although the response of cMyBP-C to mechanical load displays a complex pattern, it is highly conserved across species.

INTRODUCTION

Myosin binding protein-C (MyBP-C) is an accessory protein of muscle sarcomeres (1) that binds tightly to thick (myosin-containing) filaments and regulates the ability of myosin to interact with actin to generate force. In the heart, the cardiac isoform of MyBP-C (cMyBP-C) promotes actin and myosin interactions in response to inotropic stimuli so that cMyBP-C is necessary for enhanced cardiac contractility, for example in response to increased stimulation by catecholamines (2,3). The importance of cMyBP-C in cardiac function is further highlighted by the recognition that mutations in the gene encoding cMyBP-C, *MYBPC3,* are among the most frequent causes of inherited hypertrophic cardiomyopathy, the leading cause of sudden cardiac death in young people in the United States and a prominent cause of heart failure in older adults in diverse geographic populations across the globe (4,5). cMyBP-C is a member of the immunoglobulin (Ig) superfamily of proteins being composed of 11 Ig- or fibronectin (FNIII)-like domains with each domain numbered consecutively, C0 through C10, beginning at the N-terminus of the molecule (Fig. 1). Between neighboring domains there are linker sequences that vary in length, composition, and structure (6–8). Two of the longest linkers occur in the N-terminal half of the protein. One of them is an ~52-amino-acid-long sequence that is rich in proline and alanine residues (the P/A region) and is located between domains C0 and C1. The second is an ~105-residue-long linker called the M-domain that is located between the C1 and C2 domains. The M-domain constitutes a central regulatory motif of cMyBP-C with phosphorylation sites unique to the cardiac isoform of MyBP-C located within this region. Phosphorylation of these sites by a number of kinase reduces the ability of cMyBP-C to bind to actin (9,10) or myosin S2 (11). Domains C8–C10 at the C-terminus of the molecule bind to titin and the light meromyosin segment of myosin and are responsible for anchoring cMyBP-C to the thick filament backbone (12–14).

Additional insights into the structure of cMyBP-C were recently obtained in studies using NMR (8) and single-molecule atomic force microscopy (AFM) (15). In these studies the M-domain was shown to be partially folded and to contain intrinsically disordered sequences, whereas the P/A-rich region was predicted to be entirely disordered (15,16). Furthermore, the Ig- and FNIII-like domains of recombinant mouse cMyBP-C were found to be mechanically weaker than those of other Ig/FnIII proteins such as titin (17–19). cMyBP-C is thus suggested to be highly extensible under low loads, potentially making it well suited to function as a sarcomeric mechanosensor (20,21) or as a compliant spring-like element such as the PEVK segment of titin (22,23). Ultimately, order-disorder transitions modulated by mechanical stress, phosphorylation, or ligand binding may provide a basis for dynamic regulation of cMyBP-C structure and function during contraction.

The purpose of the current experiments was to investigate whether the general mechanical features of cMyBP-C first

Submitted November 30, 2012, and accepted for publication April 8, 2013.
*Correspondence: samharris@ucdavis.edu
Editor: Matthias Rief.

0006-3495/13/06/2465/11 $2.00
http://dx.doi.org/10.1016/j.bpj.2013.04.027

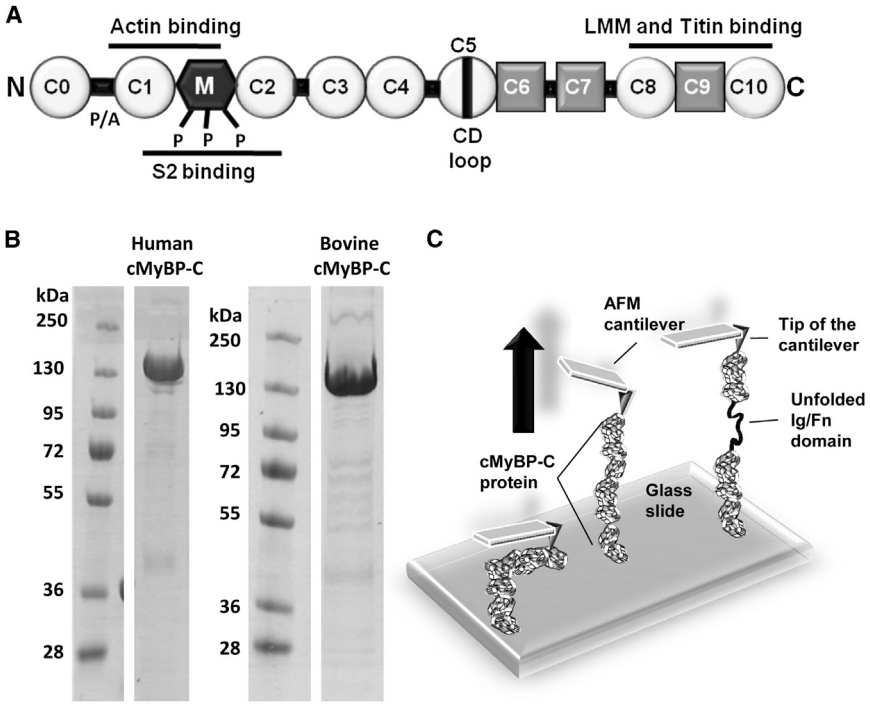

FIGURE 1 Schematic diagrams showing the domain structure of cMyBP-C and an AFM experiment. (*A*) Domain organization of cMyBP-C showing that cMyBP-C is a multidomain protein consisting of 11 Ig- (*circles*) or FNIII-like domains (*squares*) numbered C0–C10. Sequences linking the Ig/FNIII-like domains include a sequence rich in prolines and alanines (the P/A region) located between domains C0 and C1 and the regulatory M-domain (M) located between domains C1 and C2. Phosphorylation sites (P) within the M-domain are indicated. Binding sites to myosin S2 and to actin are indicated by black lines near the N-terminus of cMyBP-C. Binding sites to light meromyosin and titin are indicated by black lines near the C-terminus. (*B*) Coomassie stained SDS-PAGE of recombinant human cMyBP-C and purified native bovine cMyBP-C showing protein purity. (*C*) Schematic diagram showing mechanical load imposed on a single cMyBP-C molecule with an AFM cantilever.

identified in murine cMyBP-C are conserved across species and whether native and recombinant cMyBP-C molecules exhibit similar mechanical properties. In our previous study, we investigated the mechanical responses of mouse cMyBP-C expressed in a baculovirus/insect cell expression system (15). Here, we extended these studies by investigating the mechanical properties of recombinant human cMyBP-C expressed in a baculovirus/insect cell system and native cMyBP-C purified from bovine heart. The results show that the mechanical responses of cMyBP-C are remarkably similar across species and that native and recombinant cMyBP-C molecules display comparable properties under load. Taken together, our results establish a common mechanical fingerprint of cMyBP-C that includes hierarchical unfolding of Ig/FNIII-like domains over a range of relatively low forces (<180 pN), and the extension of compliant regions including the regulatory M-domain at forces below 50 pN.

METHODS

Protein expression and purification

A full-length human cMyBP-C cDNA was obtained by reverse transcription polymerase chain reaction, from human cardiac total RNA (Stratagene, La Jolla, CA). The cDNA (GenBank accession no. NM_000256.3) was subcloned and used for protein expression as previously described for the murine protein (15). Protein purity typically exceeded 95% as assessed with sodium dodecyl sulfate-polyacrylamide gel electrophoresis (SDS PAGE) (8% gel) (Fig. 1 *B*, *left*). Proteins were used within 1 week of preparation.

Native cMyBP-C (GenBank accession no. NP_001070004) was purified from bovine heart according to Hartzell and Glass (24) with modifications as described below. Hearts were obtained from cows freshly slaughtered at the UC Davis Department of Animal Science Meat Lab. Left ventricles were removed from the hearts, dissected free of connective tissue and fat, and ground before freezing in liquid nitrogen and stored at −80°C until further use. Throughout the purification all samples were kept on ice or at 4°C. Briefly, 65 g of fresh or thawed tissue was homogenized in a blender for 2 min. The homogenate was washed 5× in 300 ml of Buffer A containing (in mM) 50 KCl, 20 Tris-HCl, 2 EDTA, 15 2-mercaptoethanol, pH 7.9 in successive cycles of centrifugation (3000 × *g*, 15 min) and resuspension. After each centrifugation the pellet was homogenized with a Polytron homogenizer. Homogenization steps were repeated two more times using 300 ml Buffer A containing 1% Triton-X, and then five times using 300 ml Buffer A (without Triton) until the pellet became white. The pellet was then resuspended in 150 ml EDTA-PO_4 buffer containing (in mM) 10 EDTA, 124 NaH_2PO_4, 31 Na_2HPO_4 pH 5.9, and stirred for 15 min. The solution was then centrifuged (10,000 × *g*, 20 min) and the supernatant retained. The EDTA extraction was repeated once on the pellet, and the two supernatants were pooled. cMyBP-C was precipitated from the pooled supernatants by slowly adding saturated ammonium sulfate to a 45% final concentration. Precipitated cMyBP-C was collected by centrifugation (15,000 × *g*, 15 min). The pellet was dissolved in 8 ml Buffer K containing (in mM) 300 KCl, 5.2 K_2HPO_4, 4.8 NaH_2PO_4, 2 NaN_3, 0.1 EDTA, 3 2-Mercaptoethanol pH 5.9 and dialyzed against Buffer K overnight. The extract containing cMyBP-C protein was then chromatographed on a 2.5 × 35-cm column of hydroxylapatite and eluted with a pH 6.8 phosphate gradient from (in mM) 300 NaCl, 2 NaN_3, 0.1 EDTA, 3 2-mercaptoethanol, 15 NaH_2PO_4, 28 K_2HPO_4 to 300 NaCl, 1 NaN_3, 0.1 EDTA, 3 2-mercaptoethanol, 56 NaH_2PO_4, 119 K_2HPO_4. The purest fractions were pooled for experiments and used within 1 week. The purity of bovine cMyBP-C was assessed with SDS PAGE (8% gel) (Fig. 1. *B*, *right*).

AFM

AFM measurements, data inclusion criteria, and analysis procedures were performed as previously described (15). Data were obtained using an MFP3D instrument (Asylum Research, Santa Barbara, CA) housed at the

UC Davis Spectral Imaging Facility. BioLever A cantilevers (silicon nitride probe, gold coated, Olympus, Tokyo, Japan) were used to obtain force measurements and the stiffness (k) of each cantilever was calculated by measuring the thermally driven mean-square vertical bending fluctuations and applying the equipartition theorem (25). Typical cantilever stiffness was ~30 pN/nm.

Immediately before the AFM experiments, proteins were clarified by ultracentrifugation at 400,000 × g for 30 min and diluted to 20–25 μg/ml in a buffer containing (in mmol/L) 20 imidazole, 180 KCl, 1 $MgCl_2$, 1 EGTA, 1 DTT, pH 7.4. Diluted proteins (in ~100 μl volumes) were deposited by nonspecific adsorption onto cleaned glass slides. Unbound cMyBP-C was washed away after 1 min by gently rinsing the slide 5× with fresh buffer (~150 μl). Force versus extension curves were then collected by pressing the cantilever tip into the protein-coated surface and raising the cantilever tip up to 600 nm above the glass surface with a constant pulling speed (100, 500, 3000, or 5000 nm/s) to stretch a cMyBP-C molecule adhered to the cantilever tip. The experimental arrangement is shown in Fig. 1 *C*. Displacement of the cantilever base was measured by using an integrated linear voltage differential transformer. Force (F) was obtained from cantilever bending (d) according to the formula of stiffness ($F = dk$). Force-displacement curves were corrected as described previously (15). Contour length (L_c) and persistence length (L_p) values were obtained by fitting the continuous, nonlinear parts of the force traces with the worm-like chain (WLC) equation (26) using the built-in software of the Asylum AFM Instrument (Igor Pro 6.0 WaveMetrics, Portland, OR, MFP version 090909, Asylum Research, Santa Barbara, CA.).

Monte Carlo simulations

Force-driven cMyBP-C unfolding was simulated using an elastically coupled two-state model (27,28) in which the activation kinetics are influenced by the mechanical load and the shape of the unfolding potential. In the simulation a full-length cMyBP-C molecule is pulled at a constant, preadjusted velocity. The initial contour length of the molecule was set according to the number of Ig/FNIII globular domains (11 × 4 nm) and the theoretical total lengths of the unstructured regions (108, 115, and 120 nm for the human, bovine, and mouse proteins, respectively). As the chain was extended, force was generated according to the WLC equation (29). In each polling interval (dt) the probability (P_u) of domain unfolding at the given force (f) was calculated according to

$$P_u = \omega_0\, dt e^{-(E_{au} - f\Delta x_u)/k_B T}, \quad (1)$$

where ω_0 is attempt frequency set by Brownian dynamics (30), k_BT is thermal energy, E_{au} is activation energy of unfolding, and Δx_u is distance between the folded and transition states along the unfolding reaction coordinate. Domain unfolding was permitted or prohibited depending on a comparison of P with a number generated randomly between 0 and 1. Each domain unfolding event incremented the molecule's contour length by 34.2, 33.4, and 33.2 nm, which are the average unfolded protein chain lengths of the component globular domains of human, bovine, and mouse cMyBP-C, respectively. To obtain the unfolding potential width (Δx) and the unfolding activation energy (E_a) for the average globular domain of different types of cMyBP-C, iterative simulation cycles were carried out in which each of the parameters were independently changed with increments of 0.005 nm and 5 × 10^{-22} J, respectively. The unfolding forces obtained during stretch-velocity-dependent simulations were then compared with the experimental data set.

Statistics

All values represent mean ± SD.

RESULTS

Force-extension curves of recombinant and native cMyBP-C

The mechanical properties of individual human and bovine cMyBP-C molecules were investigated using single-molecule AFM. Fig. 1 *C* shows a schematic of the experiments: cMyBP-C molecules were first adsorbed onto a glass surface, and then picked at random attachment points along their contour and stretched by moving the cantilever away from the slide surface. The molecules became stretched until the load on the molecule was sufficient to mechanically unfold tertiary and secondary structures such as the β-pleated sheets of Ig-like domains. Domain unfolding events were evident as characteristic sawtooth peaks in the force-extension traces caused by the sudden drop of cantilever force as each domain unfolded causing an incremental increase in the overall molecular contour length (ΔL) (31). The height of the individual peaks marks the force in the instant of domain unfolding and depends on the mechanical stability of the domains and the loading rate. The greater the mechanical stability or the loading rate, the greater the instantaneous force and vice versa (32).

A total of 51 force-extension curves for human recombinant cMyBP-C were obtained at stretch rates ranging between 200 and 5000 nm/s. As shown in Fig. 2 *A* for a force-extension curve of a full-length human cMyBP-C molecule, the maximum number of peaks in any one spectrum was 11 (with the final, 12th peak corresponding to the detachment of the molecule from the cantilever tip or the slide surface), as predicted for the total combined number of Ig- and FNIII-like domains within a single cMyBP-C (6). In two spectra with 11 peaks the maximum measured contour lengths (L_c) were 452 and 490 nm, both in reasonable agreement with the theoretical predicted L_c of 492 nm (0.38 nm/amino acid (aa) × 1295) for a full-length molecule. Notably, the recombinant human cMyBP-C used in our experiments contained 1295 residues including a 21-aa-long His-tag and short linker sequence appended at the N-terminus to aid in protein purification. Fig. 2 *B* shows a single-molecule force-extension curve for cMyBP-C purified from bovine heart. Human and bovine cMyBP-C display ~89% sequence identity (Fig. S1 in the Supporting Material), and the gross structural arrangement of their Ig- and FNIII-like domains is similar, with 11 Ig/FNIII domains predicted for both. Consistent with this, the force-extension relationships obtained from native bovine cMyBP-C appeared very similar to those obtained from recombinant human cMyBP-C. The length of bovine cMyBP-C is predicted to be 1269 aa, yielding a maximum theoretical L_c of 482 nm (0.38 nm/aa × 1269 aa). A single force versus extension curve with 11 unfolding peaks was obtained with a contour length of 454 nm (Fig. 2 *B*).

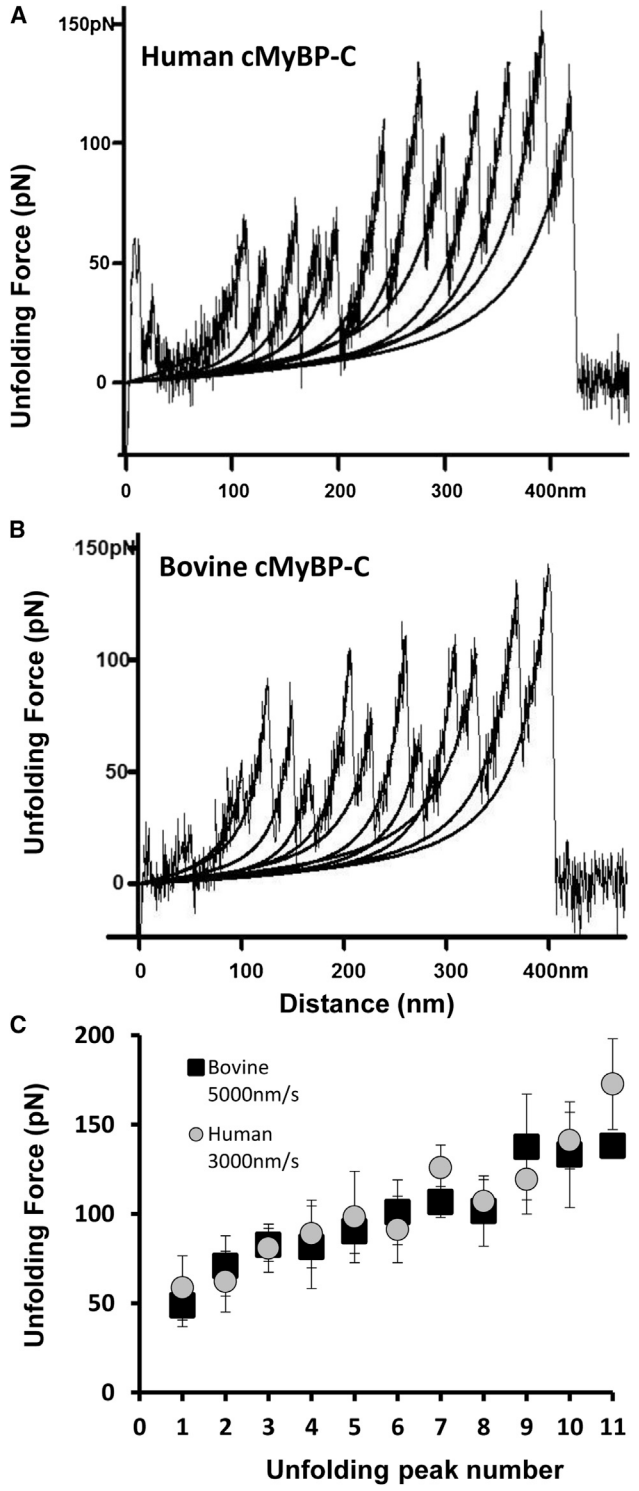

FIGURE 2 Representative force-extension curves and summary unfolding data for human and bovine cMyBP-C. Force-extension curves obtained from (*A*) recombinant human cMyBP-C and (*B*) native bovine cMyBP-C obtained at pulling speeds of 3000 and 5000 nm/s, respectively. Stretching individual cMyBP-C molecules resulted in a pattern of sawtooth peaks indicative of Ig/FNIII domain unfolding. Black lines indicate WLC model fits to the data. (*C*) Plots of unfolding force versus peak position (*peak number*) for human cMyBP-C (*gray circles*) and purified native bovine cMyBP-C (*black squares*).

Fig. 2 *C* shows summary data for the average forces required to unfold individual domains of human and bovine cMyBP-C plotted against the order of each unfolding event in a force curve. The Ig/FNIII domains of both human and bovine cMyBP-C unfolded at gradually increasing forces across a force range of ~50 to 180 pN similar to our previous results on mouse recombinant cMyBP-C (15). The three- to fourfold difference in forces required to unfold the first versus the final domains suggests that the different domains of cMyBP-C exhibit a wide range of mechanical stabilities. The average unfolding force of all domains of human cMyBP-C was 97.6 ± 31.6 pN at a pulling speed of 3000 nm/s; the average unfolding force for all bovine domains was 94.1 ± 28.8 pN at pulling speeds of 5000 nm/s.

The WLC model (26) was used to calculate the ΔL that resulted from each domain unfolding event. The average ΔL for the unfolding of all individual domains of human cMyBP-C was 32.3 ± 11.8 nm ($n = 340$). When corrected for the folded length of the domains (~4 nm) this value agrees well with the average theoretical contour lengths of the domains that are predicted to be 34.2 ± 8.7 nm using domain boundaries as determined by DomPred (33) and PONDR (34) (see Fig. S6). A histogram showing the distribution of domain contour lengths from 51 human force-extension curves with 5–11 sawtooth peaks is shown in Fig. S2. For bovine cMyBP-C the average ΔL per unfolded domains was 31.7 ± 11.3 nm ($n = 171$) (Fig. S2), which is also in reasonable agreement after correction for domain folding with the average theoretical domain contour lengths of the bovine domains (33.4 ± 8.9 nm) (33,34).

Mechanical complexity in Ig/FnIII unfolding

Fig. 3 shows several force-extension curves obtained from recombinant human and native bovine cMyBP-C. Prominent features observed in many of the force-extension plots are instances where the force required to unfold an Ig/FNIII-like domain was anomalously lower than the force required to unfold the preceding domain (*arrowheads*). Similar drops in force were also observed in force-extension plots of mouse cMyBP-C (15), but the occurrence of the force drop events in human cMyBP-C were more stereotyped than in the mouse force-extension curves. For example, Fig. 3 *A* shows three independent force curves containing 8, 9, or 10 unfolding events that were superimposed to reveal a force drop that appeared at an identical location in each of the curves. A force drop was also observed in a full-length force curve representing a completely unfolded human cMyBP-C (Fig. 3 *B*). The difference in force between the preceding peak and the dropped peak was up to 50 pN (Fig. S3); this exceeds the standard error of the average domain unfolding force and particularly the error of the position-normalized domain unfolding force (see Fig. 2 *C*). In a homogenous system, such as a homopolymer, mechanically driven

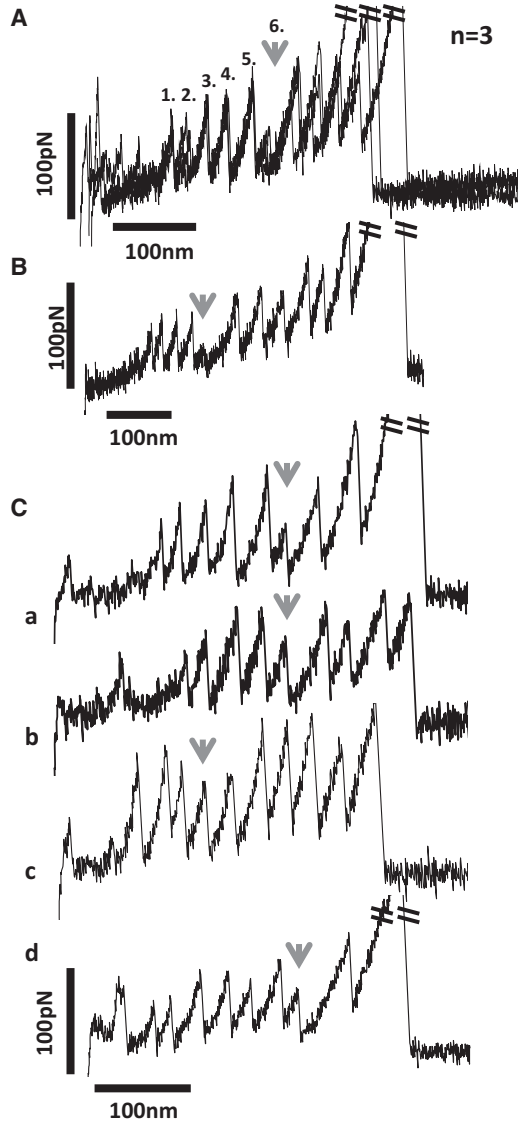

FIGURE 3 Force-extension curves showing anomalous force drops. (*A*) Three force versus extension curves obtained from human cMyBP-C in three independent experiments are shown superimposed. Each curve shows a distinct force drop at the 6th unfolding peak (*gray arrow*). (*B*) A full-length force-extension curve of a human cMyBP-C molecule. Gray arrow indicates a force drop at the 5th unfolding peak. (*C*) Example force versus extension curves for human (*a* and *b*) and bovine (*c* and *d*) cMyBP-C. Gray arrows indicate force drops at various locations.

unfolding at a constant loading rate occurs at a similar, average force for each component domain (35). However, in a heterogeneous system such as the cMyBP-C molecule, the unfolding of mechanically unstable domains precedes that of the stable ones, which unfold at progressively increasing instantaneous forces (17). Thus, in a serially linked system of interaction free domains mechanically driven unfolding follows an order set by the relative mechanical stabilities of the individual domains, resulting in a sawtooth-shaped force spectrum with gradually increasing force peaks. A large force drop is therefore unexpected, and its systematic presence likely points at structural coupling within the chain.

Force drops were also evident in force-extension plots from native bovine cMyBP-C (Fig. 3), although their position was not as systematic as for human cMyBP-C. In this respect, the frequency and positions of force drops for bovine cMyBP-C were more similar to those reported previously for mouse recombinant cMyBP-C (15). Force drops >15 pN were observed in 17 out of 35 bovine force spectra and 21 out of 51 human force spectra.

Pulling rate dependence of unfolding forces and mechanical stability of different domains

To further investigate possible differences between recombinant human and native bovine cMyBP-C molecules, the pulling rate dependence of domain unfolding events was measured. Fig. 4 shows histogram distributions of domain unfolding forces for human and bovine cMyBP-C Ig/FNIII domains at pulling rates of 500, 3000, and 5000 nm/s. Fig. 4 *A* (*inset*) shows a histogram of unfolding force for human cMyBP-C measured at 200 nm/s pulling rate. For both human and bovine cMyBP-C the mean unfolding force and the width of the unfolding force distribution increased as expected with increased pulling rate (17,18,32). The mean unfolding forces for recombinant human cMyBP-C were 77.9 ± 27 pN, 97.6 ± 31.6 pN, and 103.3 ± 32.5 pN at pulling rates of 500, 3000, and 5000 nm/s, respectively. The mean unfolding forces for native bovine cMyBP-C were 74.5 ± 17.2 pN, 89.2 ± 28.2 pN, and 94.8 ± 28.3 pN at pulling rates of 500, 3000, and 5000 nm/s, respectively.

Fig. 5 shows a cross-species comparison of the average unfolding forces for human, mouse, and bovine cMyBP-C plotted against pulling rate. Data for the recombinant mouse cMyBP-C were reprinted from (15) and are included here to facilitate comparisons. Notably, all cMyBP-C molecules exhibited similar mechanical stabilities at loading rates of 500, 3000, and 5000 nm/s, but bovine and human cMyBP-C showed a weak trend for lower mechanical stability relative to mouse cMyBP-C at the highest pulling speeds. The slopes of the human and bovine relationships were also similar and slightly less steep than the mouse relationship. Differences between human and bovine cMyBP-C were not significant at any pulling speed.

Monte Carlo simulations of mechanically driven cMyBP-C unfolding

To reveal the equilibrium unfolding activation kinetics and characterize the shape of the unfolding potentials, Monte Carlo simulations (Fig. S4) were carried out and compared with experimental data. Fig. 5 shows results from the Monte Carlo simulations (*straight lines*) superimposed over the experimental data of mean unfolding forces obtained at

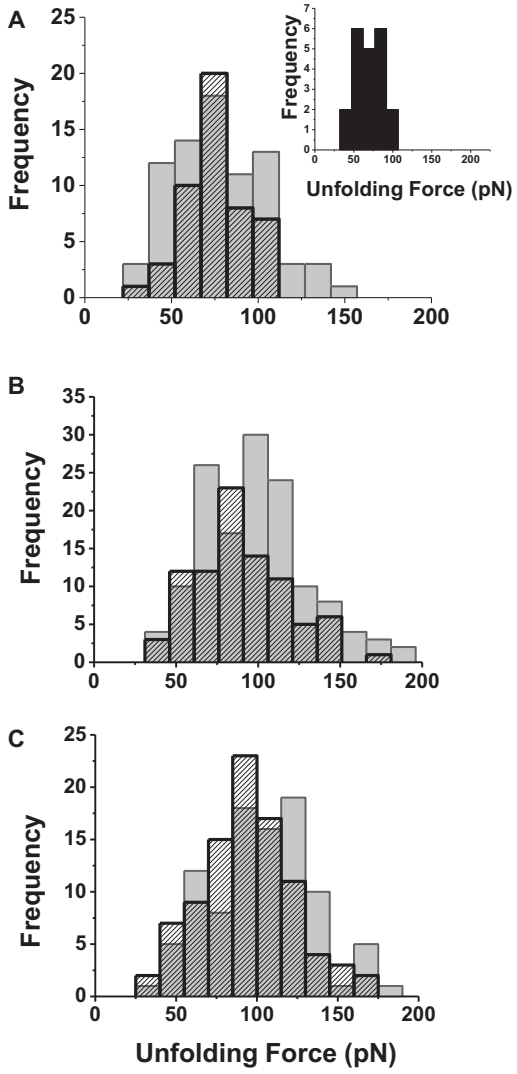

FIGURE 4 Pulling rate dependence of unfolding forces for human and bovine cMyBP-C. Unfolding-force distributions of cMyBP-C from human (*gray bars*) and bovine (*black contours*) are shown at pulling rates of (*A*) 500 nm/s, (*B*) 3000 nm/s, and (*C*) 5000 nm/s. Inset in *A* shows unfolding force of human cMyBP-C at 200 nm/s pulling rate.

pulling rates of 500, 3000, and 5000 nm/s (mouse data from (15)). Best fits to the data were obtained with activation energy and unfolding potential width values of 16.4 kcal/mol and 0.53 nm, 15.53 kcal/mol and 0.42 nm, and 14.7 kcal/mol and 0.315 nm for bovine, human, and mouse cMyBP-C, respectively (see Table 2). Fig. 6 summarizes the data by displaying the unfolding potentials for the three cMyBP-C orthologs. Notably, the greater the activation barrier, the greater the width of the unfolding potential and vice versa. Thus, although bovine cMyBP-C is thermodynamically the most stable among the different cMyBP-C molecules, because of the shape of its unfolding potential, it will unfold most easily at pulling rates exceeding 100 nm/s. Conversely, although the mouse cMyBP-C is the least thermodynamically stable, because of the shape of its unfolding potential,

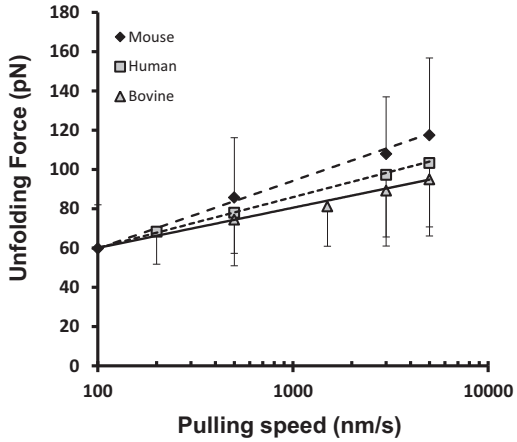

FIGURE 5 Cross-species comparisons of pulling rate dependence of mean unfolding forces for cMyBP-C Ig/FNIII domains. The pulling speed dependence for the average unfolding forces of recombinant human and native bovine cMyBP-C are shown plotted at various pulling speeds and compared to recombinant mouse cMyBP-C. Data for recombinant mouse cMyBP-C were replotted from (15) to facilitate comparisons with human and bovine cMyBP-C. Solid and dashed lines are Monte Carlo simulation fits for human, bovine, and mouse cMyBP-C shown superimposed over the experimental data.

at pulling rates exceeding 100 nm/s it will display the greatest mechanical stability among the three proteins. Conceivably, tuning the unfolding potential width could function as an adaptive mechanism to reinforce mechanical stability at high pulling rates.

Extensibility of cMyBP-C at low forces

A characteristic feature of force-extension curves determined previously from recombinant mouse cMyBP-C was

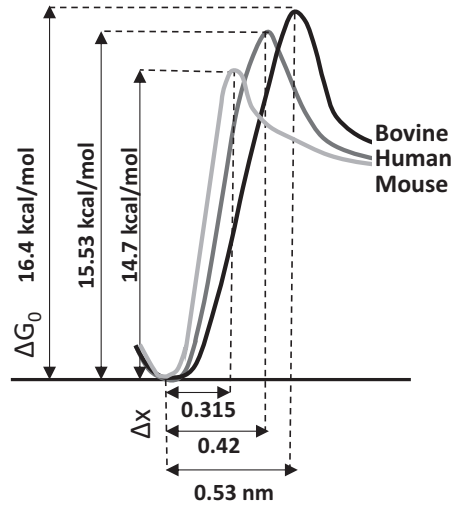

FIGURE 6 Unfolding potential diagrams from Monte Carlo simulations. Potential diagrams were drawn using activation energy (ΔG_0) and unfolding potential width (Δx) parameters obtained from Monte Carlo simulations for the three different (*human*, *bovine*, and *mouse*) cMyBP-C proteins.

the presence of a variable length ($Lc = 137.4 \pm 25$ nm) extensible segment located at the beginning of the force-extension traces (15). The segment was evident as a gradual rise in force up to ~50 pN before Ig/FNIII domain unfolding events that were seen as regularly spaced sawtooth peaks. For a force-extension curve obtained from a fully unfolded cMyBP-C molecule, the length of this initial feature presumably includes the contour length of the fully straightened cMyBP-C molecule (e.g., for a full-length molecule this could be ≈ 44 nm $= 11$ domains $\times$ 4 nm/domain) and extension of the mechanically weakest segment(s) of the protein such as unstructured or instrinsically disordered linker sequences or segments with secondary structure that are not otherwise folded into stable tertiary structures. For mouse cMyBP-C, we showed that the M-domain contributed to the extensible segment of the force-extension spectra (15) in good agreement with NMR data (8), which demonstrated the M-domain consists of disordered sequences along with three α-helices arranged in a compact bundle.

Fig. 7 shows the initial extensible segments from two recombinant human cMyBP-C molecules and summary data of L_c and L_p values obtained from WLC fits of the initial portions of human and bovine cMyBP-C force-extension curves. Similar to the mouse data (15), the histogram of contour lengths for the extensible segments of human cMyBP-C (Fig. 7 *B*) showed a broad distribution of lengths from 71–186 nm with an average L_c of 129.2 $\pm$ 25.8 nm (from 35 spectra with an average number of 7 peaks). The L_p values for the human cMyBP-C also showed a broad variation from 0.33 to 2.6 nm with an average of 0.83 $\pm$ 0.51 ($n = 35$). For bovine cMyBP-C the L_c distribution of the extensible region featured a single Gaussian distribution between 75 and 173 nm with an average L_c of 105.1 $\pm$ 23.4 nm (Fig. 7 *B*). The average L_p of bovine cMyBP-C was 0.79 $\pm$ 0.51 nm ($n = 18$ spectra with an average of 7 peaks) and ranged from 0.21 to 1.85 nm (Fig. 7 *C*). The broad distribution observed for both the contour lengths and persistence lengths likely reflects variations in the site of cantilever attachment in different cMyBP-C molecules and is consistent with the idea that multiple linker segments with variable lengths and secondary structures contribute to responses of cMyBP-C to stretch under load as for titin's PEVK region (37).

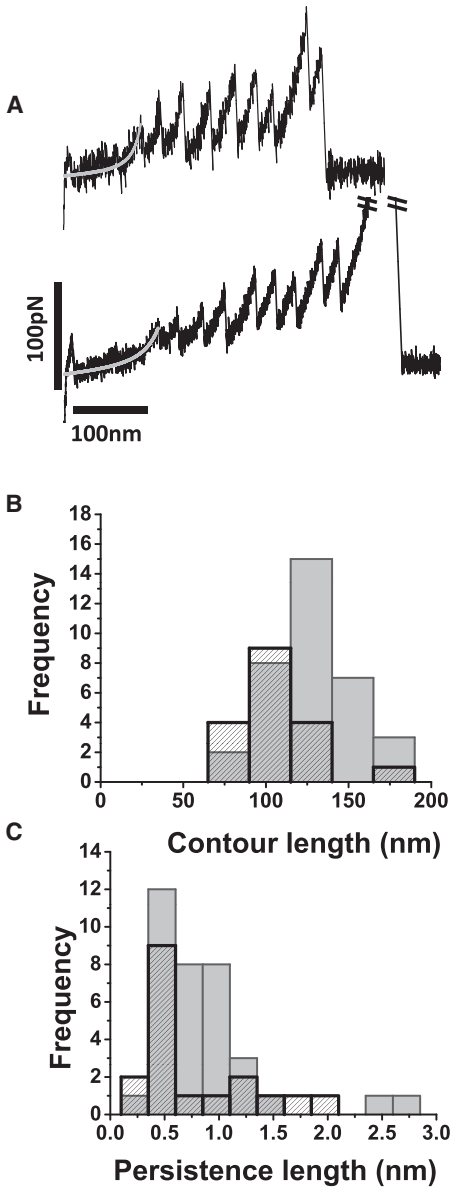

FIGURE 7 Low-compliance extensible segments of human cMyBP-C. (*A*) Two representative force versus extension curves for human cMyBP-C showing variable lengths of the initial extensible segments. WLC fits to the extensible segments are shown in gray. (*B*) Histogram of the contour length distribution of the extensible regions of human (*dashed bars*) (129.2 $\pm$ 25.8 nm, $n = 35$) and bovine cMyBP-C (*gray bars*) (105.1 $\pm$ 23.4 nm, $n = 18$). (*C*) Histogram of the persistence length distribution of human (*dashed bars*) (0.83 $\pm$ 0.51 nm, $n = 35$) and bovine (*gray bars*) (0.79 $\pm$ 0.51 nm, $n = 18$) cMyBP-C.

DISCUSSION

We recently determined the characteristic mechanical properties of individual cMyBP-C molecules by using AFM on proteins expressed from a mouse cMyBP-C cDNA (15). In this study we extended these experiments to include orthologous cMyBP-C molecules from different species using proteins obtained from both native and recombinant sources. The main conclusion from this study is that the overall mechanical response of individual cMyBP-C molecules is complex, representing multiple distinct contributions from both compliant and stably folded sequences, however the mechanical signature of cMyBP-C is highly conserved across species from mouse to human. Collectively, our results thus establish a characteristic mechanical fingerprint common to cardiac MyBP-C molecules. The common features of cMyBP-C from the different sources include a pronounced, overall highly hierarchical unfolding

of Ig and FNIII domains, a systematic pattern of unfolding events including stereotyped events that are suggestive of structural coupling between domains, and the presence of multiple elastic segments that together can be extended to lengths exceeding 100 nm by forces smaller than ~50 pN. These low-force extensible segments probably include sequences with little or no tertiary structure such as intrinsically disordered sequences and partially folded helices (8,38–40) such as those occurring in the M-domain. Details revealed by dynamic force spectroscopy suggest that the different domain stabilities of cMyBP-C can provide an adaptive mechanism that aids in avoiding extensive domain unfolding at high loading rates.

Conserved mechanical features of cMyBP-C

The finding that the general mechanical features of cMyBP-C are conserved across different species is consistent with the high degree of sequence similarity (~89% identity) of bovine and mouse cMyBP-C sequences compared to human cMyBP-C (Fig. S1). The high degree of sequence identity includes the Ig/FNIII domains that typically share >90% identity suggesting that there is a strong selection pressure to maintain the physical properties and functions of the individual Ig/FNIII domains at each unique position along the length of a cMyBP-C molecule. This high degree of sequence conservation is especially striking given that relatively few amino acids are necessary for the determination of the overall mechanical stability of an Ig β-fold (41). By comparison, neighboring Ig/FnIII domains within a single cMyBP-C molecule are far less conserved with the most similar domains being ~33% identical (Fig. S1 *B*). The lack of similarity between adjacent domains most likely underlies the mechanical heterogeneity observed leading to the wide range of stabilities of the different domains within a single cMyBP-C molecule (Fig. 2 *C*). An analogous lack of sequence similarity was also noted among the Ig domains of titin's I-band that also display a mechanical unfolding hierarchy and that could be grouped into strong and weak families (41,42). By comparison to these domains, all of the cMyBP-C unfolding events belong to the weak category (unfolding at loads <200 pN) making them more similar to actin cross-linking proteins such as filamin A (43) rather than the mechanically strong Ig domains of titin or myomesin (17,39,44,45).

In comparing the overall stabilities of Ig/FNIII domains across the different species (Fig. 5), there was a weak trend that the mouse domains unfolded at higher forces than either the human or bovine domains, although the differences were not statistically significant. However, results from Monte Carlo simulations (Fig. 6 and Fig. S4), indicated that the order of stability was reversed among the species-specific cMyBP-C orthologs under conditions of zero load. That is, the order of thermodynamic stability when $F = 0$ was bovine > human > mouse, whereas under dynamic loading conditions (>100 nm/s) it reversed to mouse > human > bovine. The phenomenon is attributed to the shape of the unfolding potential (Fig. 6), according to which the width of the unfolding potential is smallest for the mouse and largest for the bovine cMyBP-C (see Table 2). Although under unloaded conditions ($F = 0$) only the height of the activation barrier determines the spontaneous domain unfolding rate, under dynamic loading conditions the shape of the unfolding potential also strongly influences the process such that the smaller the width of the unfolding potential, the greater the loading-rate dependence of unfolding forces and vice versa. In the beating heart if cMyBP-C molecules are attached to the thick and thin filaments at the same time (46,47), they are then exposed to dynamic loading conditions. It is an intriguing question whether domain unfolding could occur under the in situ loading conditions. Considering the physiological cardiac sarcomere length range (1.6–2.2 μm (48)) and species-specific heart rates (average 540, 80, and 60 beats per minute in mouse, human, and bovine heart, respectively (49),) we obtain pulling rates of ~5500, ~800, and ~600 nm/s for mouse, human, and bovine sarcomeres, respectively. At these loading rates, unless high instantaneous forces (>80 pN) are reached, the domains of cMyBP-C are likely to resist mechanical unfolding in all of the species investigated.

Another common feature revealed by our cross-species study was the frequent appearance of force drops in cMyBP-C force-extension plots (Fig. 3). The occurrence of low-force peaks interspersed between high-force sawtooth peaks was previously described in force spectra of *Dictyostelium* filamin molecules (43). In that study, the reduced force peaks were attributed to a stable unfolding intermediate in one of the Ig domains that resulted in a two-step unfolding profile. Considering that these two-step unfolding events resulted in partial contour-length gains (less than the ΔL expected for a complete Ig/FNIII domain), whereas the sawtooth peak spacing was uniform in our measurements (Fig. S5), it is unlikely that the force drops observed during the mechanical unfolding of cMyBP-C molecules were caused by partial domain unfolding intermediates. Rather, a structural circumstance, such as coupling between domains, could impose a determinant order on the sequence of domain unfolding events. In the case of cMyBP-C there is indeed evidence for associations among the different Ig domains (e.g., C5 and C8) (50), and cMyBP-C appears U or V shaped in electron microscope images (51,52) suggesting that additional structural coupling or stable geometries may be present between domains.

A long extensible segment with variable length and morphology was another prominent feature of all cMyBP-C force-extension curves. The segment typically occupied ~16–20% of the total molecular L_c and was apparent before

the appearance of the more regular sawtooth peaks indicative of Ig/FNIII domain unfolding events. The contour lengths of the human and bovine extensible segments were not significantly different, but the measured length of the bovine segment appeared slightly shorter than the human (105.1 ± 23.4 vs. 129.2 ± 25.8 nm, respectively). The difference may reflect the additional length of the His-tag linker sequence at the N-terminus of the recombinant human cMyBP-C. Consistent with this possibility, the L_c of the extensible segment of mouse cMyBP-C (137.4 ± 25 nm), which also includes an expressed N-terminal His-tag, was similar to that of the human cMyBP-C (15). The persistence lengths (L_p) of the extensible segments were similar in cMyBP-C molecules from the different species (Tables 1 and 2).

The sequences that contribute to the low-force extensible segment of cMyBP-C most likely include ones that link the Ig/FNIII domains together, such as the sequence rich in proline and alanine residues located between C0 and C1 (~52 aa), the regulatory M-domain that links C1 and C2 (~105 aa), and other shorter sequences between each Ig/FNIII domain. Computational algorithms predict that many of these linker segments lack significant secondary or tertiary structure and have a propensity for intrinsic disorder (Fig. S6). For instance, the proline-alanine sequences of all three cMyBP-C isoforms are predicted to be almost entirely disordered. This sequence is also the least conserved of the different isoforms studied (~46% identity). We previously noted that sequence differences in this region contribute to an inverse relationship between the percentage of proline and alanine residues in the segment and the heart rate in mammals, suggesting that the proline-alanine segment could potentially contribute to fine-tuning of the contractile apparatus (53). Although the AFM results presented here did not reveal systematic differences in the mechanical properties of the extensible segments of species with different heart rates (e.g., mouse and human), it is possible that changes in its mechanical properties would not be detected because the P/A region accounts for only ~20 nm (52 aa × 0.38 nm/aa) of the total length of the extensible segment.

The M-domain is another sequence that is predicted to be only partially ordered, thereby contributing to the low-force extensible segment of cMyBP-C force-extension curves (15). We previously showed using AFM that the M-domain of a mouse recombinant cMyBP-C exhibited nonlinear elastic behavior and concluded that, in contrast to earlier predictions based on small-angle x-ray scattering data (54), it fails to fold into a stable Ig-like configuration. In support of the AFM data, recent NMR data also showed that the M-domain consists of an unstructured sequence at its N-terminus, which includes the phosphorylatable serines followed by a more structured region that is folded into a bundle of three α-helices (8). The trihelix bundle contains a consensus sequence for actin binding (8) and has recently been shown to bind calmodulin in the presence of calcium (55). Because the M-domain is extensible at low forces, it is an intriguing possibility that modulation of ligand binding could occur via a mechanical opening or extension of the trihelix bundle under conditions of load thereby exposing cryptic binding sites within the trihelix motif. Furthermore, because phosphorylation often induces disorder-to-order transitions (or vice versa) (56,57), phosphorylation could alter the mechanical properties of the M-domain and potentially affect the stability of the trihelix bundle (58). If so, then at least some of the variability observed in the L_p and L_c values of the extensible segments of the force-extension spectra may be due to heterogeneity in the phosphorylation states of native and recombinant proteins (59,60).

Physiological significance

This study used AFM to determine the single-molecule mechanical properties of cMyBP-C from different species using native and genetically expressed proteins. Together with previous results from recombinant mouse cMyBP-C (15), this study establishes a common mechanical fingerprint for cMyBP-C that is well conserved across multiple species. Although the precise arrangement of cMyBP-C within the sarcomere is not yet known, there is accumulating evidence that cMyBP-C spans the interfilament space between thick and thin filaments (46) and that it interacts with actin through multiple binding sites in its N-terminal domains (9,46,61–65). If so, then the mechanical stability of cMyBP-C may be important in fine-tuning the dynamics of the interaction between these filamentous systems in sarcomeres (23). Furthermore, the presence of low-force extensible segments within cMyBP-C may provide a mechanism for chemically modulated elastic coupling between the

TABLE 1 Summary data of mechanical properties of human, bovine, and mouse cMyBP-C

		Human cMyBP-C	Bovine cMyBP-C	Mouse cMyBP-C
Extensible region	L_c (nm)	129.21 ± 25.8 (n = 35)	105.1± 23 3 (n = 18)	137.4 ± 25 (n = 17)
	L_p (nm)	0.83 ± 0.51 (n = 35)	0.79 ± 0.51 (n = 18)	0.65 ± 031 (n = 17)
Ig/FnIII domains	L_c (nm)	32.3 ± 11.8 nm (n = 320)	31.7 ± 11.3 (n = 214)	33.3 ± 15.4 (n = 155)
Unfolding force at different pulling speed (pN)	500 nm/s	77.9 ± 27 (n = 79)	74.5 ± 17.2 (n = 49)	83.2 ± 30 (n = 149)
	3000 nm/s	97.6 ± 31.6 (n = 138)	89.2 ± 28.2 (n = 87)	106.7 ± 31.5 (n = 26)
	5000 nm/s	103.3 ± 32.5 (n = 96)	94.8 ± 28.3 (n = 93)	117.5 ± 39.3 (n = 79)

Data for mouse cMyBP-C was reprinted from (15). Abbreviations: L_c, contour length; L_p, persistence length.

TABLE 2 Kinetic parameters obtained from Monte Carlo simulations

	Kinetic parameters	Human cMyBP-C	Bovine cMyBP-C	Mouse cMyBP-C
Monte Carlo simulation	ΔG (kcal/mol)	15.53	16.4	14.7
	Δx (nm)	0.42	0.53	0.315

ΔG is the calculated free energy barrier between the folded and unfolded state at zero force, Δx is the distance between the folded state and the transition state along the unfolding reaction coordinate (i.e., width of the unfolding potential).

contractile filaments that can respond to the temporally and spatially localized demands during a single heart beat.

SUPPORTING MATERIAL

Six figures, legends, and references (66–68) are available at http://www.biophysj.org/biophysj/supplemental/S0006-3495(13)00460-8.

The authors thank Elaine Hoye and Camelia Dumitras for their expert technical assistance in cloning and purification of recombinant human cMyBP-C, Alan Hicklin for his technical help at the Spectral Imaging Facility of University of California, Davis, and Attila Nagy for helpful discussions and comments on an earlier version of the manuscript.

This work was supported by grants from the National Institutes of Health (NIH) (HL080367) to S.P.H. and from the Hungarian Science Foundation (OTKA K84133) to M.K.

REFERENCES

1. Offer, G., C. Moos, and R. Starr. 1973. A new protein of the thick filaments of vertebrate skeletal myofibrils. Extractions, purification and characterization. *J. Mol. Biol.* 74:653–676.
2. Stelzer, J. E., J. R. Patel, and R. L. Moss. 2006. Protein kinase A-mediated acceleration of the stretch activation response in murine skinned myocardium is eliminated by ablation of cMyBP-C. *Circ. Res.* 99:884–890.
3. Tong, C. W., J. E. Stelzer, …, R. L. Moss. 2008. Acceleration of crossbridge kinetics by protein kinase A phosphorylation of cardiac myosin binding protein C modulates cardiac function. *Circ. Res.* 103:974–982.
4. Xu, Q., S. Dewey, …, A. V. Gomes. 2010. Malignant and benign mutations in familial cardiomyopathies: insights into mutations linked to complex cardiovascular phenotypes. *J. Mol. Cell. Cardiol.* 48:899–909.
5. Harris, S. P., R. G. Lyons, and K. L. Bezold. 2011. In the thick of it: HCM-causing mutations in myosin binding proteins of the thick filament. *Circ. Res.* 108:751–764.
6. Yasuda, M., S. Koshida, …, T. Obinata. 1995. Complete primary structure of chicken cardiac C-protein (MyBP-C) and its expression in developing striated muscles. *J. Mol. Cell. Cardiol.* 27:2275–2286.
7. Guardiani, C., F. Cecconi, and R. Livi. 2008. Stability and kinetic properties of C5-domain from myosin binding protein C and its mutants. *Biophys. J.* 94:1403–1411.
8. Howarth, J. W., S. Ramisetti, …, P. R. Rosevear. 2012. Structural insight into unique cardiac myosin-binding protein-C motif: a partially folded domain. *J. Biol. Chem.* 287:8254–8262.
9. Shaffer, J. F., R. W. Kensler, and S. P. Harris. 2009. The myosin-binding protein C motif binds to F-actin in a phosphorylation-sensitive manner. *J. Biol. Chem.* 284:12318–12327.
10. Weith, A., S. Sadayappan, …, D. M. Warshaw. 2012. Unique single molecule binding of cardiac myosin binding protein-C to actin and phosphorylation-dependent inhibition of actomyosin motility requires 17 amino acids of the motif domain. *J. Mol. Cell. Cardiol.* 52:219–227.
11. Gautel, M., O. Zuffardi, …, S. Labeit. 1995. Phosphorylation switches specific for the cardiac isoform of myosin binding protein-C: a modulator of cardiac contraction? *EMBO J.* 14:1952–1960.
12. Moos, C., G. Offer, …, P. Bennett. 1975. Interaction of C-protein with myosin, myosin rod and light meromyosin. *J. Mol. Biol.* 97:1–9.
13. Flashman, E., H. Watkins, and C. Redwood. 2007. Localization of the binding site of the C-terminal domain of cardiac myosin-binding protein-C on the myosin rod. *Biochem. J.* 401:97–102.
14. Gilbert, R., M. G. Kelly, …, D. A. Fischman. 1996. The carboxyl terminus of myosin binding protein C (MyBP-C, C-protein) specifies incorporation into the A-band of striated muscle. *J. Cell Sci.* 109:101–111.
15. Karsai, A., M. S. Kellermayer, and S. P. Harris. 2011. Mechanical unfolding of cardiac myosin binding protein-C by atomic force microscopy. *Biophys. J.* 101:1968–1977.
16. Jeffries, C. M., Y. Lu, …, J. Trewhella. 2011. Human cardiac myosin binding protein C: structural flexibility within an extended modular architecture. *J. Mol. Biol.* 414:735–748.
17. Rief, M., M. Gautel, …, H. E. Gaub. 1997. Reversible unfolding of individual titin immunoglobulin domains by AFM. *Science.* 276:1109–1112.
18. Carrion-Vazquez, M., A. F. Oberhauser, …, J. M. Fernandez. 1999. Mechanical and chemical unfolding of a single protein: a comparison. *Proc. Natl. Acad. Sci. USA.* 96:3694–3699.
19. Li, H., M. Carrion-Vazquez, …, J. M. Fernandez. 2000. Point mutations alter the mechanical stability of immunoglobulin modules. *Nat. Struct. Biol.* 7:1117–1120.
20. Lammerding, J., R. D. Kamm, and R. T. Lee. 2004. Mechanotransduction in cardiac myocytes. *Ann. N. Y. Acad. Sci.* 1015:53–70.
21. Gautel, M. 2011. Cytoskeletal protein kinases: titin and its relations in mechanosensing. *Pflugers Arch.* 462:119–134.
22. Linke, W. A., M. Kulke, …, J. M. Fernandez. 2002. PEVK domain of titin: an entropic spring with actin-binding properties. *J. Struct. Biol.* 137:194–205.
23. Anderson, B. R., and H. L. Granzier. 2012. Titin-based tension in the cardiac sarcomere: molecular origin and physiological adaptations. *Prog. Biophys. Mol. Biol.* 110:204–217.
24. Hartzell, H. C., and D. B. Glass. 1984. Phosphorylation of purified cardiac muscle C-protein by purified cAMP-dependent and endogenous Ca2+-calmodulin-dependent protein kinases. *J. Biol. Chem.* 259:15587–15596.
25. Hutter, J. L., and J. Bechhoefer. 1993. Calibration of atomic-force microscope tips. *Rev. Sci. Instrum.* 64:1868–1873.
26. Bustamante, C. 1994. Probing biological surfaces. *Science.* 264:296.
27. Rief, M., J. M. Fernandez, and H. E. Gaub. 1998. Elastically coupled two-level systems as a model for biopolymer extensibility. *Phys. Rev. Lett.* 81:4764–4767.
28. Kellermayer, M. S., C. Bustamante, and H. L. Granzier. 2003. Mechanics and structure of titin oligomers explored with atomic force microscopy. *Biochim. Biophys. Acta.* 1604:105–114.
29. Bustamante, C., J. F. Marko, …, S. Smith. 1994. Entropic elasticity of lambda-phage DNA. *Science.* 265:1599–1600.
30. Bell, G. I. 1978. Models for the specific adhesion of cells to cells. *Science.* 200:618–627.
31. Carrion-Vazquez, M., A. F. Oberhauser, …, J. M. Fernandez. 2000. Mechanical design of proteins studied by single-molecule force spectroscopy and protein engineering. *Prog. Biophys. Mol. Biol.* 74:63–91.
32. Oberhauser, A. F., C. Badilla-Fernandez, …, J. M. Fernandez. 2002. The mechanical hierarchies of fibronectin observed with single-molecule AFM. *J. Mol. Biol.* 319:433–447.
33. Bryson, K., D. Cozzetto, and D. T. Jones. 2007. Computer-assisted protein domain boundary prediction using the DomPred server. *Curr. Protein Pept. Sci.* 8:181–188.

34. Radivojac, P., Z. Obradović, …, A. K. Dunker. 2003. Prediction of boundaries between intrinsically ordered and disordered protein regions. *Pac. Symp. Biocomput.* 216–227.

35. Evans, E., and K. Ritchie. 1999. Strength of a weak bond connecting flexible polymer chains. *Biophys. J.* 76:2439–2447.

36. Reference deleted in proof.

37. Li, H., A. F. Oberhauser, …, J. M. Fernandez. 2001. Multiple conformations of PEVK proteins detected by single-molecule techniques. *Proc. Natl. Acad. Sci. USA.* 98:10682–10686.

38. Sarkar, A., S. Caamano, and J. M. Fernandez. 2005. The elasticity of individual titin PEVK exons measured by single molecule atomic force microscopy. *J. Biol. Chem.* 280:6261–6264.

39. Schoenauer, R., P. Bertoncini, …, I. Agarkova. 2005. Myomesin is a molecular spring with adaptable elasticity. *J. Mol. Biol.* 349:367–379.

40. Nagy, A., L. Grama, …, M. S. Kellermayer. 2005. Hierarchical extensibility in the PEVK domain of skeletal-muscle titin. *Biophys. J.* 89:329–336.

41. Garcia, T. I., A. F. Oberhauser, and W. Braun. 2009. Mechanical stability and differentially conserved physical-chemical properties of titin Ig-domains. *Proteins.* 75:706–718.

42. Li, H., W. A. Linke, …, J. M. Fernandez. 2002. Reverse engineering of the giant muscle protein titin. *Nature.* 418:998–1002.

43. Schwaiger, I., A. Kardinal, …, M. Rief. 2004. A mechanical unfolding intermediate in an actin-cross-linking protein. *Nat. Struct. Mol. Biol.* 11:81–85.

44. Rief, M., M. Gautel, and H. E. Gaub. 2000. Unfolding forces of titin and fibronectin domains directly measured by AFM. *Adv. Exp. Med. Biol.* 481:129–136, discussion 137–141.

45. Marszalek, P. E., H. Lu, …, J. M. Fernandez. 1999. Mechanical unfolding intermediates in titin modules. *Nature.* 402:100–103.

46. Luther, P. K., H. Winkler, …, J. Liu. 2011. Direct visualization of myosin-binding protein C bridging myosin and actin filaments in intact muscle. *Proc. Natl. Acad. Sci. USA.* 108:11423–11428.

47. Luther, P. K., and R. Craig. 2011. Modulation of striated muscle contraction by binding of myosin binding protein C to actin. *Bioarchitecture.* 1:277–283.

48. Hibberd, M. G., and B. R. Jewell. 1982. Calcium- and length-dependent force production in rat ventricular muscle. *J. Physiol.* 329:527–540.

49. Reece, W. O. 2009. Functional Anatomy and Physiology of Domestic Animals. Wiley-Blackwell, Hoboken, NJ.

50. Moolman-Smook, J., E. Flashman, …, H. Watkins. 2002. Identification of novel interactions between domains of Myosin binding protein-C that are modulated by hypertrophic cardiomyopathy missense mutations. *Circ. Res.* 91:704–711.

51. Hartzell, H. C. 1985. Effects of phosphorylated and unphosphorylated C-protein on cardiac actomyosin ATPase. *J. Mol. Biol.* 186:185–195.

52. Swan, R. C., and D. A. Fischman. 1986. Electron microscopy of C-protein molecules from chicken skeletal muscle. *J. Muscle Res. Cell Motil.* 7:160–166.

53. Shaffer, J. F., and S. P. Harris. 2009. Species-specific differences in the Pro-Ala rich region of cardiac myosin binding protein-C. *J. Muscle Res. Cell Motil.* 30:303–306.

54. Jeffries, C. M., A. E. Whitten, …, J. Trewhella. 2008. Small-angle X-ray scattering reveals the N-terminal domain organization of cardiac myosin binding protein C. *J. Mol. Biol.* 377:1186–1199.

55. Lu, Y., A. H. Kwan, …, J. Trewhella. 2012. The motif of human cardiac myosin-binding protein C is required for its Ca2+-dependent interaction with calmodulin. *J. Biol. Chem.* 287:31596–31607.

56. Bright, J. N., T. B. Woolf, and J. H. Hoh. 2001. Predicting properties of intrinsically unstructured proteins. *Prog. Biophys. Mol. Biol.* 76:131–173.

57. Müller-Späth, S., A. Soranno, …, B. Schuler. 2010. From the Cover: Charge interactions can dominate the dimensions of intrinsically disordered proteins. *Proc. Natl. Acad. Sci. USA.* 107:14609–14614.

58. Michalek, A. J., J. W. Howarth, …, D. M. Warshaw. 2013. Phosphorylation modulates the mechanical stability of the cardiac myosin-binding protein C motif. *Biophys. J.* 104:442–452.

59. Ge, Y., I. N. Rybakova, …, R. L. Moss. 2009. Top-down high-resolution mass spectrometry of cardiac myosin binding protein C revealed that truncation alters protein phosphorylation state. *Proc. Natl. Acad. Sci. USA.* 106:12658–12663.

60. Copeland, O., S. Sadayappan, …, S. B. Marston. 2010. Analysis of cardiac myosin binding protein-C phosphorylation in human heart muscle. *J. Mol. Cell. Cardiol.* 49:1003–1011.

61. Lu, Y., A. H. Kwan, …, C. M. Jeffries. 2011. The C0C1 fragment of human cardiac myosin binding protein C has common binding determinants for both actin and myosin. *J. Mol. Biol.* 413:908–913.

62. Orlova, A., V. E. Galkin, …, J. Trewhella. 2011. The N-terminal domains of myosin binding protein C can bind polymorphically to F-actin. *J. Mol. Biol.* 412:379–386.

63. Mun, J. Y., J. Gulick, …, R. Craig. 2011. Electron microscopy and 3D reconstruction of F-actin decorated with cardiac myosin-binding protein C (cMyBP-C). *J. Mol. Biol.* 410:214–225.

64. Rybakova, I. N., M. L. Greaser, and R. L. Moss. 2011. Myosin binding protein C interaction with actin: characterization and mapping of the binding site. *J. Biol. Chem.* 286:2008–2016.

65. Kensler, R. W., J. F. Shaffer, and S. P. Harris. 2011. Binding of the N-terminal fragment C0-C2 of cardiac MyBP-C to cardiac F-actin. *J. Struct. Biol.* 174:44–51.

66. Huang, X., and W. Miller. 1991. A time-efficient, linear-space local similarity algorithm. *Adv. Appl. Math.* 12:337–357.

67. Pearson, W. R., and D. J. Lipman. 1988. Improved tools for biological sequence comparison. *Pro. Nat. Acad. Sci.* 85:2444–2448.

68. Romero, P. 2001. Sequence complexity of disordered protein. *Proteins.* 42:38–48.